Separation of screened Coulomb interaction and phase-space filling in exciton bleaching of multiple quantum wells

Koo-Chul Je,[1,2] Moongoo Choi,[2] Sang-Youp Yim,[2] Jeung Sun Ahn,[1] and Seung-Han Park[2]
[1]*Japan Advanced Institute of Science and Technology, Ishikawa 923-1211, Japan*
[2]*Institute of Physics and Applied Physics, and Department of Physics, Yonsei University, Seoul 120-749, Korea*
(Received 26 February 2002; revised manuscript received 24 June 2002; published 4 October 2002)

Excitonic nonlinearity in multiple quantum wells due to many-body interactions consisting of phase-space filling and screened Coulomb interaction is investigated. In particular, we show that the effects of the screened Coulomb interaction and the phase-space filling on the exciton bleaching can be separated for highly excited carrier densities by femtosecond pump pulses. We also find that the phase-space filling effects on the excitonic bleaching are about three times larger than the effects of screened Coulomb interaction and gradually decreases with increasing carrier density within the Mott density.

DOI: 10.1103/PhysRevB.66.155312 PACS number(s): 73.21.Fg, 71.35.Cc, 78.67.De

The confinement of an electron and a hole in semiconductor multiple quantum wells (MQW's) provides strong optical nonlinearities[1,2] that may be useful for applications to integrated optics, optical switching devices, optical logic gates, or even optical data processing.[3,4] The optical nonlinearities have been explained by the bleaching, shift and broadening of the excitonic absorption resonance due to many-body (MB) interactions that include the Pauli exclusion principle, long-range Coulomb screening (CS), and band-gap renormalization. The exclusion principle can be divided into the phase-space filling (PSF) and the exchange effects, which are very short ranged compared to the screened Coulomb (SC) interaction. We denote both effects as PSF, including the exchange effects. The relative contribution of the PSF and CS effects to the optical nonlinearities had been intensively investigated by variations of excitonic absorption spectra. Many groups have found that the PSF effects are more effective than the screening effect in significant excitonic absorption changes in MQW's.[1,5–9] However, to our knowledge, there was no report on the separation of the PSF and CS effects in 1 hh and 2 hh excitons for the highly excited carrier densities in MQW's.

In this paper, we propose a method to find the relative strength of the PSF and CS effects in the optical excitonic nonlinearities by investigating the variations of bleaching and broadening of exciton peaks in the first and second subbands for excited carrier densities of the femtosecond pulses in a GaAs/AlGaAs MQW.

In photoexcited MQW's, by femtosecond pump pulses at the lowest exciton resonance, one can observe the absorption spectrum including exciton peaks in the first (1 hh) and second (2 hh) subbands. Almost all the excited carriers occupy the first subband and few carriers can occupy the second subband due to the short spectral width of the pump pulse. This proposed system can be more clearly realized when picosecond or nanosecond pump pulses are utilized due to its very narrow spectral width. The carrier density in the second subband can be increased, as the strength of pump pulse increases. However, it is very small relative to the excited density of the first subband. If the carriers are excited only for the first subband, we can assume that the changes of 1 hh exciton peak are related to the combination of the PSF and CS effects and various scattering events, that is, carrier-carrier and carrier-phonon collisions due to the occupied e-h pairs in the first subband.

In contrast, the changes of the 2 hh exciton peak result only from the pure CS induced by the occupied e-h pairs. It can be read from a inset in Fig. 1, where the variations of the 2 hh exciton peak without the SC effects are almost constant in the excited density limit. Thus, subtracting the variation rate of 2 hh excitonic peak from the variation rate of the 1 hh excitonic peak at low temperature, we can obtain the variation induced only by the PSF effects including the scattering effects. The included scattering effects mainly affect the broadening of exciton resonance. In order to investigate the scattering effects, we calculate the variations of the 1 hh exciton resonance without the SC effects. In this case, the broadening is almost constant and the bleaching is very weak in our density limit. Therefore, we can see that the other scattering effects except the PSF and SC effects are very weak in the excitonic variations within the density limit. Therefore, it is possible to distinguish these two different mechanisms by systematically investigating the excitonic variations associated with different subbands.

Since the energy gap between first and second subbands is about 100 meV, we should consider the effects of carriers in the second subband induced by femtosecond pump pulses to distinguish the two different mechanisms. In other word, the variation of 2 hh exciton peak contains the PSF effect due to excited carrier density from a pump pulse. If we want to extract the pure PSF effects induced by the excited carrier density in the first subband, we should subtract the 2 hh exciton variations from the 1 hh exciton variations. Through the similar processes, we can make complete separation of the screening and the PSF effects in the nonlinear optical response for various carrier densities in the MQW's.

Our calculations are based on the multiband-semiconductor Bloch equations (MSBE) for the electron (hole) distribution functions $f^{e}_{i,\mathbf{k}}(f^{h}_{j,\mathbf{k}})$ in band i (j) and the corresponding interband polarizations $P_{ji,\mathbf{k}}$. The MSBE can be written as[10,11]

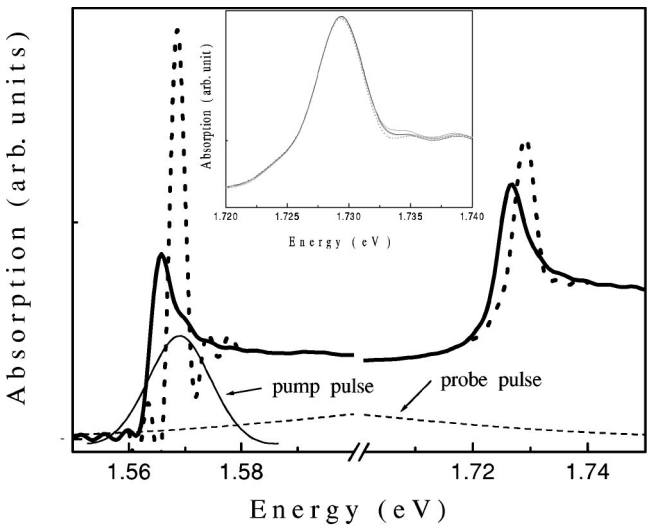

FIG. 1. Dotted curve shows the absorption spectrum without the pump pulse and the solid curve is nonlinear absorption spectrum with a excited carrier density 2.3×10^{10} cm^{-2} by the pump pulse at 10 K. The pump pulse is tuned at the 1 hh exciton resonance and the probe pulse covers the two exciton peaks. The inset shows the 2 hh exciton peaks for various carrier densities within 2.3×10^{10} cm^{-2} without the CS effects.

$$\frac{\partial}{\partial t}P_{ji,\mathbf{k}}=\frac{1}{i\hbar}\sum_{i'j'}(\mathcal{E}^{e}_{ii',\mathbf{k}}\delta_{jj'}+\mathcal{E}^{h}_{jj',-\mathbf{k}}\delta_{ii'})P_{j'i',\mathbf{k}}+\frac{1}{i\hbar}\sum_{i'j'}\mathcal{U}_{i'j',\mathbf{k}}(\delta_{ii'}\delta_{jj'}-\delta_{jj'}f^{e}_{i,\mathbf{k}}-\delta_{ii'}f^{h}_{j,-\mathbf{k}})+\left.\frac{\partial P_{ji,\mathbf{k}}}{\partial t}\right|_{inco},$$

$$\frac{\partial}{\partial t}f^{e}_{i,\mathbf{k}}=\frac{1}{i\hbar}\sum_{j'}(\mathcal{U}_{ij',\mathbf{k}}P^{*}_{j'i,\mathbf{k}}-\mathcal{U}^{*}_{ij',\mathbf{k}}P_{j'i,\mathbf{k}})+\left.\frac{\partial f^{e}_{i,\mathbf{k}}}{\partial t}\right|_{inco},$$

$$\frac{\partial}{\partial t}f^{h}_{j,-\mathbf{k}}=\frac{1}{i\hbar}\sum_{i'}(\mathcal{U}_{i'j,\mathbf{k}}P^{*}_{ji',\mathbf{k}}-\mathcal{U}^{*}_{i'j,\mathbf{k}}P_{ji',\mathbf{k}})+\left.\frac{\partial f^{h}_{i,-\mathbf{k}}}{\partial t}\right|_{inco}, \quad (1)$$

where

$$\mathcal{U}_{ij,\mathbf{k}}=\mu_{ij,\mathbf{k}}E(t)-\sum_{i'j',\mathbf{k}'}V^{eh}_{s}\left(\begin{smallmatrix}\mathbf{k}-\mathbf{k}'-\mathbf{k}\mathbf{k}'\\ i\quad j'\quad j\,i'\end{smallmatrix}\right)P_{j'i',\mathbf{k}'} \quad (2)$$

and

$$\mathcal{E}^{e}_{ii',\mathbf{k}}=\epsilon^{e}_{i,\mathbf{k}}\delta_{ii'}-\sum_{i'',\mathbf{k}''}V^{ee}_{s}(^{\mathbf{k}\mathbf{k}''\mathbf{k}\mathbf{k}''}_{ii''i'i''})f^{e}_{i'',\mathbf{k}''}$$

$$\mathcal{E}^{h}_{jj',\mathbf{k}}=\epsilon^{h}_{j,\mathbf{k}}\delta_{jj'}-\sum_{j'',\mathbf{k}''}V^{hh}_{s}(^{\mathbf{k}\mathbf{k}''\mathbf{k}\mathbf{k}''}_{j'j''jj''})f^{h}_{j'',\mathbf{k}''}. \quad (3)$$

$\mathcal{U}_{ij,\mathbf{k}}$'s are renormalized Rabi frequencies and $\mathcal{E}^{e}_{ii',\mathbf{k}}(\mathcal{E}^{h}_{jj',\mathbf{k}})$'s are renormalized electron (hole) energies.[10] $\mu_{ij,k}$ is an optical dipole matrix element between conduction bond (i) and valence band (j) states and $\epsilon^{e(h)}_{i(j),k}$ are the electron(hole) single-particle energies that are calculated with the Kronig-Penney model. $E(t)$ is the optical field for the combined pump and probe laser pulses. V_s denotes the matrix elements of the screened Coulomb potential. The collision terms denoted by $(\cdots)|_{inco}$ are calculated beyond the Hartree-Fock approximation and especially electron-LO-phonon couplings are considered up to second order with the well-known Markov approximation at low temperature. The coupling contributes to dephasing of interband polarizations as well as energy-relaxation processes.[11] Here, $\vec{k}$ denotes the momentum associated with the relative motion of electrons and holes.

The field renormalization and the band-gap renormalization are affected also by the screening effects through Coulomb potential. The Coulomb enhancement term, which is strongly affected by the screened Coulomb potential, within the single-plasmon pole approximation can be written as[12]

$$V_{s}\left(\begin{smallmatrix}\mathbf{k}-\mathbf{k}'-\mathbf{k}\mathbf{k}'\\ i\quad j'\quad j\,i'\end{smallmatrix}\right)=\frac{2\pi e^{2}}{\epsilon_{0}L^{2}}\frac{1}{(\vec{k}-\vec{k}')+\kappa(n,T)}, \quad (4)$$

where n is the plasma density ($n=2\Sigma_{i,\mathbf{k}}f_{i,\mathbf{k}}$) and ϵ_0 is background dielectric constant. $\kappa(n,T)$ is the inverse screening length of the Coulomb potential and depends on n and temperature T. The inverse of the screening length is calculated self-consistently according to $\kappa^2=(2\pi e^2/\epsilon_0 V)\Sigma_n[df_n(k)/d\varepsilon]$.[13] Since the κ modifies the strength of Coulomb interaction, it plays a quantitatively important role in the optical excitonic nonlinearities. The 2 hh exciton depends strongly on the interband polarization $P_{22}(t)(=\Sigma_k\mu^{*}_{22,k}P_{22,k})$, which is hardly affected by the PSF effects induced by the resonantly excited carriers at the 1 hh resonance.

For simplicity model, the collision terms were taken by a simple dephasing time that is of the order of 0.5 ps, and we have ignored the light hole states and used a GaAs/AlGaAs MQW with 75-Å well width and 100-Å barrier in the theoretical calculation model.

Figure 1 shows the calculated linear and nonlinear absorption spectra for a carrier density of 2.3×10^{10} cm^{-2} created by a 200-fs pump pulse that is tuned in the 1 hh exciton resonance at 10 K. The solid and dotted curves are the absorption spectra with and without the pump pulse of 1.568 eV at 1 hh exciton peak, respectively. The 1 hh and 2 hh exciton peaks with the pump pulse show redshift and their oscillator strengths are also strongly bleached by the competition of the PSF and the CS effects. This redshift is explained in the Fig. 3. The shifts of both exciton peaks are almost similar, but the 1 hh excitonic bleaching is significantly stronger than the 2 hh excitonic bleaching which originates almost from the screened Coulomb correction due to excited carriers. The PSF effects are also included in the 2 hh excitonic variation, but they are very weak. The inset figure shows the 2 hh exciton peaks for various excited carrier densities within 2.3×10^{10} cm^{-2}, without the Coulomb screening effect. The 2 hh exciton peaks are hardly changed and are almost independent of the carrier density. Also, we have found that, in particular, 1 hh exciton broadenings are

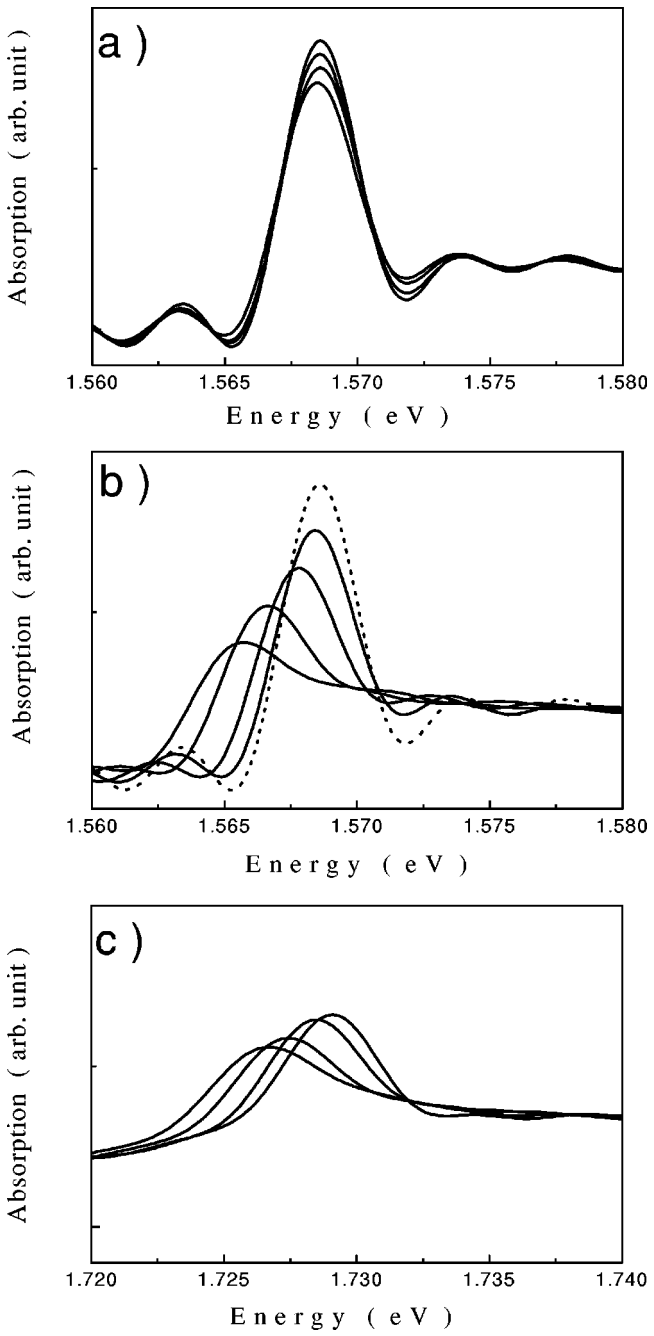

FIG. 2. Absorption spectra for various carrier densities in the MQW at 10 K. The carrier densities are from the top curve (a) 6.5×10^{6}, 3.7×10^{7}, 1.1×10^{8}, 3.2×10^{8} cm^{-2}; (b) from right curve 5.1×10^{8}, 2.9×10^{9}, 1.1×10^{10}, 2.3×10^{10} cm^{-2}; and (c) from right curve 5.6×10^{6}, 3.5×10^{7}, 8×10^{8}, 3.1×10^{8} cm^{-2}. The dotted curve corresponds to the without pump pulse.

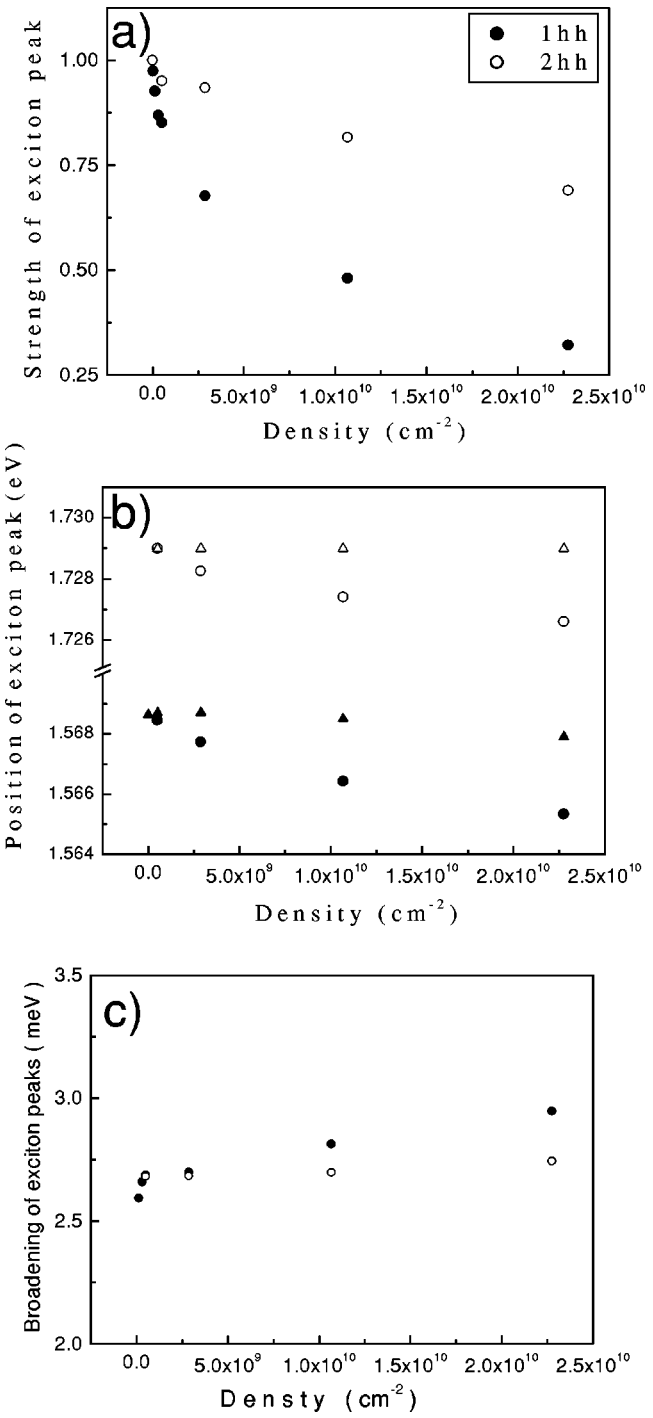

FIG. 3. (a) Strength of the 1 *hh* and 2 *hh* exciton peaks, (b) their energy positions in the presence and in the absence of the SC effects, and (c) broadening of the 1 *hh* exciton peak as a function of the carrier densities. The strengths are normalized by the 1 *hh* exciton peak without the pump pulse.

hardly changed with a weak bleaching in the density limit as shown in the Fig. 3. The redshift of the 1 *hh* exciton peaks are caused by the SC effects in our model. Therefore, we can assume that the major part of the 2 *hh* excitonic bleaching is directly caused by the CS effects and pure broadening of the 2 *hh* exciton resonance may be the dominant bleaching mechanism. As the 2 *hh* variations are subtracted from the 1 *hh* variations induced by the combined PSF and screened Coulomb correction, we obtain the pure PSF effect in the optical excitonic nonlinearity. Consequently, we can separate the PSF effects and the screened Coulomb correction effects for the optical excitonic nonlinearity in the quantum wells.

Figure 2 shows absorption spectra for various carrier densities in the MQW at 10 K. Figure 2(a) displays the 1 *hh* exciton peaks at various carrier densities of 6.5×10^{6}, 3.7

$\times 10^7$, 1.1×10^8, and 3.2×10^8 cm^{-2}. It shows the bleaching of excitonic oscillator strengths induced by the excited carriers. The excitonic resonances are hardly shifted in these low densities. The Figs. 2(b) and 2(c) show the peaks of the 1 *hh* and 2 *hh* excitons with different strengths of pump pulses. It can be seen that the bleaching of the 1 *hh* exciton peak is larger than that of the 2 *hh* exciton peak due to more dominant PSF effects in the first subband. The excited carrier densities for the first subband are 5.1×10^8, 2.9×10^9, 1.1×10^{10}, and 2.3×10^{10} cm^{-2}. Simultaneously, the carrier densities for the second subband are 5.6×10^6, 3.5×10^7, 8×10^7, and 3.1×10^8 cm^{-2}, which are about the same densities as those obtained in Fig. 2(a). Thus, we assume that the variations of exciton peaks with low carrier densities are almost the same as the variations of 2 *hh* exciton peaks due to the PSF effects. Since the peaks in the Fig. 2(a) do not shift, the shift of the 2 *hh* exciton peak results from mainly the CS effects by the occupied carrier densities in the first subband. As mentioned above, the variations of 2 *hh* exciton peaks include the screening effect induced by the excited carriers into the first subband and in addition the many-body effects due to carriers of the second subband. It is quite similar to the many-body effects presented in the Fig. 2(a). Therefore, we can obtain only the screening effect in the first subband by subtracting the already calculated 1 *hh* exciton peak from the variations of the 2 *hh* exciton peak. Again, the PSF effects in the 1 *hh* excitonic variations in the first subband can be obtained by eliminating the measured screening effect from the 1 *hh* excitonic variations as shown in the Fig. 2(b).

Figure 3(a) shows the strengths of the 1 *hh* and 2 *hh* exciton peaks for various photoexcited carrier densities. The strengths are normalized by the exciton peaks without the pump pulse and decrease with increasing carrier densities. The strength of the 1 *hh* exciton peak especially decreases rapidly in low carrier densities. For the 2 *hh* exciton, it linearly decreases as the carrier density increases. Consequently, the bleaching of the 1 *hh* exciton peak is larger than that of the 2 *hh* exciton peak, because the 2 *hh* exciton is influenced only by screening effect due to the occupied carriers in the first subband and the 1 *hh* exciton is affected by both PSF and screening effects. The fast decrease of 1 *hh* exciton peak in low carrier densities results from the additional PSF effects. Therefore, we can see that both mechanisms make exciton peaks bleach.

Figure 3(b) shows the peak positions of the 1 *hh* and 2 *hh* exciton resonances for different carrier densities. For each carrier densities of the first and second subbands, the 1 *hh* and 2 *hh* exciton peaks are obtained from one absorption spectrum. The open and solid triangles show the peak positions in the absence of the CS effects. In this case, the 2 *hh* peaks with the solid triangles do not shift, but the 1 *hh* peaks with the open triangles first have blue shift and very low redshift with increasing carrier densities. Therefore, the redshift of the 2 *hh* exciton peak is due to the screening of carrier density in the first subband, and the shift of the 1 *hh* exciton peak is due to the combined CS and PSF effects. Both exciton peaks have stronger redshifts with increasing carrier density and their shifts have similar magnitude. Since

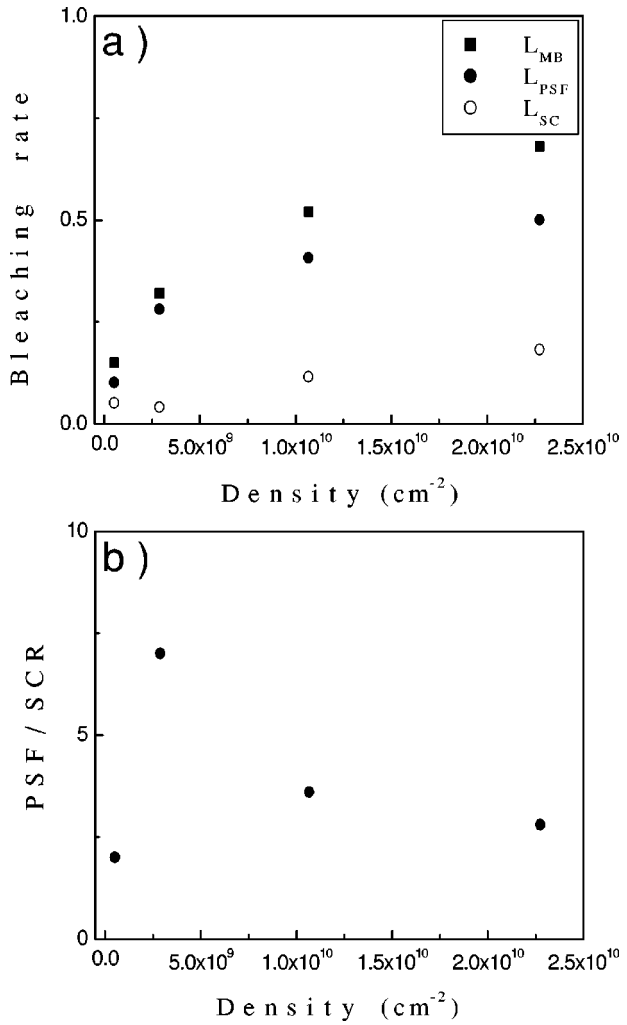

FIG. 4. (a) Excitonic bleaching rate associated with the PSF (L_{PSF}), the screening (L_{CS}), and their combined many-body (L_{MB}) effects; (b) the bleaching rate between the PSF and the screening effects as a function of the carrier densities.

the exciton-exciton interactions are not included in our calculations, the redshift of the exciton resonances appears more strongly. It means that effects of the PSF for excitonic shift are very small in these carrier densities. Consequently, the PSF effects are dominant for the excitonic bleaching, but they do not affect the excitonic shift.

Figure 3(c) shows the broadening of the 1 *hh* exciton peaks for various carrier densities in the presence and in the absence of the SC effects. Since in the absence of the SC effects the 1 *hh* exciton peaks are hardly broadened with increasing carrier density as shown with the open circle. In the presence of the SC effects the broadening of the 1 *hh* exciton peaks increase with increasing carrier densities. Therefore, we can assume that the broadening results from the bleaching of the 1 *hh* exciton peak induced by the combined PSF and SC effects and the collision terms hardly affect the excitonic broadening in the density limit.

Figure 4 shows the excitonic bleaching as L_{CS}, L_{PSF}, and L_{MB} induced in the 1 *hh* exciton peaks, and bleaching

rate L_{PSF}/L_{CS} for various carrier densities at 10 K. Here, $L_i \equiv (X_1 - X_2)/X_2$, where i denote the CS, PSF, and MB and X_1 (X_2) denotes the oscillator strength of the 1 hh (2 hh) exciton peak. Thus, the L_{CS}, L_{MB}, and L_{PSF} denote the bleaching rate of the exciton peak due to the CS, many-body, and PSF effects, respectively.

As shown in the Fig. 4(a), the L_{MB} is larger than the L_{SC} and the L_{PSF}. In addition, we can observe that L_{CS} increases slowly. Since influences of the CS will be about the same in the 1 hh and 2 hh excitons, we can estimate the bleaching induced by the only PSF effects, $L_{PSF} = L_{MB} - L_{CS}$. The L_{PSF} increases first rapidly in low densities and afterward amounts to 70–85 % of the many-body effects with increasing carrier densities. The considerable change of the 1 hh exciton peak in the absorption spectrum gives strong evidence that the PSF effects are more dominant than the screening effect[1,7] for the excitonic bleaching in the MQW.

The Fig. 4(b) shows the excitonic bleaching rate for different carrier densities. The bleaching due to the PSF effects is about 2.5–6 times larger than that due to the CS effect within the carrier densities 2.3×10^{10} cm^{-2}. It is smaller than the reported value of the highly doped MQW, in which the effects of the PSF are about ten times stronger than the effects of the screening.[14] The bleaching rate is very large in low carrier densities due to the very weak L_{CS}. The L_{PSF} increases slowly in the high carrier density, whereas the L_{CS} linearly increases and will be saturated. However, the rate gradually decreases within these carrier densities and approaches very slowly to 3 with increasing carrier densities. The rapid change of the absorption coefficient associated the first subband strongly indicates that the PSF and the exchange are more dominant than the screening effect. It is found that the PSF effects are about three times more dominant than the screened Coulomb correction effects in the excitonic nonlinearity.

In summary, we show that both the PSF and the CS mechanisms in the excitonic optical nonlinearities in the MWQ can be independently investigated by comparing the variations of the 1 hh and 2 hh exciton peaks. The screening effect for the excitonic bleaching in the MQW occupies 20–30 % of the many-body effects as carrier density increases. The PSF effects for the excitonic bleaching are about three times more dominant than the CS effect and gradually decreases with increasing carrier density. Therefore, the PSF effects are dominant mechanism for the variations of the 1 hh exciton peak, i.e., the nonlinear optical responses within the Mott density of the MQW.

ACKNOWLEDGMENTS

This work is supported by the BK 21 Project, Ministry of Science and Technology, the Advanced Backbone IT Technology Development Project (IMT 2000-B4-1), Ministry of Information, and Communication, and the Japan Society for the Promotion of Science (JSPS).

[1] S. Schmitt-Rink, D.S. Chemla, and D.A.B. Miller, Phys. Rev. B **32**, 6601 (1985).
[2] D.S. Chemla and D.A.B. Miller, J. Opt. Soc. Am. B **2**, 1155 (1985).
[3] D.A.B. Miller, D.S. Chemla, T.C. Damen, T.H. Wood, C.A. Burrus, Jr., A.C. Gossard, and W. Wiegmann, IEEE J. Quantum Electron. **21**, 1462 (1985).
[4] H. Haug, *Optical Nonlinearities and Instabilities in Semiconductors* (Academic Press, Boston, 1988).
[5] Sarah Bolton, Gregg Sucha, Daniel Chemla, D.L. Sivco, and A.Y. Cho, Phys. Rev. B **58**, 16 326 (1998).
[6] K. Litvinenko, D. Birkedal, V.G. Lyssenko, and J.M. Hvam, Phys. Rev. B **59**, 10 255 (1999).
[7] K.-H. Schlaad, C. Weber, J. Cunningham, C.V. Hoof, G. Borghs, G. Weimann, W. Schlapp, H. Nickel, and C. Klingshirn, Phys. Rev. B **43**, 4268 (1991).
[8] D.R. Wake, H.W. Yoon, J.P. Wolfe, and H. Morkoc, Phys. Rev. B **46**, 13 452 (1992).
[9] S. Hunsche, K. Leo, H. Kurz, and K. Köhler, Phys. Rev. B **49**, 16 565 (1994).
[10] H. Haug and S. W. Koch, *Quantum Theory of the Optical and Electronic Properties of Semiconductors* (World Scientific, Singapore, 1994).
[11] F. Rossi, T. Meier, P. Thomas, S.W. Koch, P.E. Selbmann, and E. Molinari, Phys. Rev. B **51**, 16 943 (1995).
[12] H. Haug and C. Ell, Phys. Rev. B **46**, 2126 (1992).
[13] K.-C. Je, T. Meier, F. Rossi, and S.W. Koch, Appl. Phys. Lett. **67**, 2978 (1995); K.-C. Je, K-C. Seo, and Yup Kim, J. Appl. Phys. **86**, 6196 (1999).
[14] D. Huang, H.Y. Chu, Y.C. Chang, R. Houdre, and H. Morkoc, Phys. Rev. B **38**, 1246 (1988).